Microfluidics Approach to Investigate the Role of Dynamic Similitude in Osteocyte Mechanobiology

Kevin Middleton [1], Avinash Kondiboyina,[2] Michael Borrett,[3] Yi Cui,[4] Xueting Mei,[4] Lidan You[1,4]

[1]Institute of Biomaterials and Biomedical Engineering, University of Toronto, 164 College Street, Room 407, Toronto, Ontario M5S 3G9, Canada, [2]Division of Engineering Science, University of Toronto, 40 Saint George Street, Room 2110, Toronto, Ontario M5S 2E4, Canada, [3]Department of Biochemistry, McMaster University, 1280 Main Street West, Room 4N59, Hamilton, Ontario L8S 4L8, Canada, [4]Department of Mechanical and Industrial Engineering, University of Toronto, 5 King's College Road, Room 105, Toronto, Ontario M5S 3G8, Canada

Received 1 May 2017; accepted 6 October 2017
Published online 6 October 2017 in Wiley Online Library (wileyonlinelibrary.com). DOI 10.1002/jor.23773

ABSTRACT: Fluid flow is an important regulator of cell function and metabolism in many tissues. Fluid shear stresses have been used to level the mechanical stimuli applied in vitro with what occurs in vivo. However, these experiments often lack dynamic similarity, which is necessary to ensure the validity of the model. For interstitial fluid flow, the major requirement for dynamic similarity is the Reynolds number (*Re*), the ratio of inertial to viscous forces, is the same between the system and model. To study the necessity of dynamic similarity for cell mechanotransduction studies, we investigated the response of osteocyte-like MLO-Y4 cells to different *Re* flows at the same level of fluid shear stress. Osteocytes were chosen for this study as flows applied in vitro and in vivo have *Re* that are orders of magnitude different. We hypothesize that osteocytes' response to fluid flow is *Re* dependent. We observed that cells exposed to lower and higher *Re* flows developed rounded and triangular morphologies, respectively. Lower *Re* flows also reduced apoptosis rates compared to higher *Re* flows. Furthermore, MLO-Y4 cells exposed to higher *Re* flows had stronger calcium responses compared to lower *Re* flows. However, by also controlling for flow rate, the lower *Re* flows induced a stronger calcium response; while degradation of components of the osteocyte glycocalyx reversed this effect. This work suggests that osteocytes are highly sensitive to differences in *Re*, independent of just shear stresses, supporting the need for improved in vitro flow platforms that better recapitulate the physiological environment. © 2017 Orthopaedic Research Society. Published by Wiley Periodicals, Inc. J Orthop Res 36:663–671, 2018.

Keywords: osteocytes; reynolds number; mechanobiology; calcium imaging; dynamic similarity

Many types of cells (e.g., endothelial cells[1] and bone cells[2]) are constantly subjected to, and respond to, fluid flow physiologically. In vitro, researchers typically investigate cellular response to different levels of fluid shear stresses (FSS).[3–5] Other fluid flow parameters, such as flow rate,[6,7] flow profile type,[8–10] and oscillatory frequency[3] have also been investigated. These parameters can be varied by increasing the syringe pump stroke length, changing the loading frequency,[3] using different flow profiles,[9] or changing the viscosity of the fluid.[6] These studies suggest that these parameters can also affect cellular responses to fluid flow stimulation. However, one group of important flow parameters, the dimensionless numbers that define the dynamic property of the fluid flow environment, has yet to be carefully examined.

One of these parameters is the Reynolds number, *Re*, which is the ratio of inertial forces (fluid momentum) to viscous forces (fluid friction). Furthermore, *Re* can be described as the ratio of dynamic pressure to shearing stresses, as defined by Equation (1).

$$Re = \frac{(\rho V)V}{\frac{\mu V}{D_H}} = \frac{\rho V D_H}{\mu} \quad (1)$$

Where ρ is the fluid density, V is the fluid velocity, D_H is the hydraulic diameter, and μ is the fluid dynamic viscosity. In addition to being a parameter of flow, *Re* also determines whether or not a fluidic model has dynamic similarity with the system it is modeling. The use of dynamic similarity in fluidic modeling is well established in the aerospace and naval industry. However, this important factor has yet to be incorporated in most in vitro fluid models. Anderson et al.[11] pioneered investigating the importance of dynamic similarity in a scaled physical model to measure the osteocyte pericellular space permeability. Nevertheless, many biological systems involve fluid flow occurring at different magnitudes of *Re* than is investigated in vitro. As such, it has not been determined whether cells are sensitive to modifications to the specific flow environment due to changes in *Re*, and whether this concept of dynamic similarity should also be applied to biological fluid models.

In this study, we investigated the response of osteocytes in different flow environment with different *Re*. Osteocytes are terminally differentiated bone cells that are sensitive to various mechanical stimuli, including FSS.[3,8,12] Osteocytes are embedded within the bone matrix in the lacunar-canalicular system (LCS). When a load is applied to bone the bone matrix is compressed, driving fluid flow within the LCS, and applying FSS to the osteocytes.[2] This stimulation modifies osteocyte signal expression and behavior,

Conflicts of interest: None.
Grant sponsor: Natural Sciences and Engineering Research Council; Grant sponsor: Toronto Musculoskeletal Centre; Grant sponsor: Barbara and Frank Milligan; Grant sponsor: Canadian Institutes of Health Research; Grant number: 282723; Grant sponsor: Canada Foundation for Innovation and the Ontario Research Fund.
Correspondence to: Lidan You (T: +416-978-5736; F: 416-978-7753; E-mail: youlidan@mie.utoronto.ca)

Table 1. Calculation of In Vivo and In Vitro *Re*

Physiological	$D_H = D_o - D_i$ (nm)		V_{avg} (μm/s)	μ (10^{-3} Pa · s)	ρ (kg/m^3)	*Re*
Canaliculi	155[17]		60[16]	1.06[a]	1025[a]	0.9×10^{-5}
Flow chamber	*W* (mm)	*H* (mm)	*Q*[b] (ml/min)	μ (10^{-3} Pa · s)	ρ (kg/m^3)	*Re*
Jacobs et al.[9]	10	0.28	18	1.06	1025	56
Li et al.[3]	38	0.28	14–141	1.06	1025	12–118
Kulkarni et al.[15]	24	0.3	20.4	1.06	1025	27

[a]Assume value for salt water. [b]Flow rates calculated from shear stresses provided by labs.

which has major implications on the mechanical properties and homeostasis of bone.[13,14]

To study specific osteocyte responses to FSS, many in vitro studies have been performed using parallel plate flow chambers (PPFC)[3,8,12,15] at physiologically measured FSS.[16] However, the fluid flow applied to the cells is not necessarily physiological as the *Re* applied in PPFCs are typically 10–120, while the *Re* in the canaliculi is $\sim 10^{-5}$ (Table 1).[3,9,15–17] We speculate that this difference in dimensional flow environment can affect the cellular response. For example, this could explain the observation of osteocytes in situ having more calcium oscillations compared to osteocytes in vitro when exposed to similar levels of FSS.[10,18,19] Therefore, we hypothesize that osteocytes respond differently to different *Re* controlled flow environments, even when FSS is kept constant.

In this study, we applied different *Re* flows to osteocytes while keeping the FSS level the same by using microfluidic devices with varying channel dimensions. We analyzed the effect that different flow environments, as controlled by the *Re*, had on osteocytes with respect to changes in cell morphology, cytoskeleton organization, apoptosis, and intracellular calcium response. Although numerous studies have been utilized to investigate cellular responses to different flow parameters by modifying microfluidic channel dimensions,[20–22] this is the first time that *Re* has been investigated as one of the important parameters of the flow environment applied to osteocytes. This work is important in determining whether dynamic similarity and dimensionality should be taken into account when developing future in vitro fluid models, and could be applied to other cells that are studied using PPFCs, such as endothelial cells.

MATERIALS AND METHODS

Device Design and Fabrication

Different channel heights, *h*, and widths, *w*, (Fig. 1A) were used to change the hydraulic diameter of the microfluidic channel. To keep wall FSS, τ_w (Equation 2) constant between devices, flow rates, *Q*, and/or the dynamic viscosity were adjusted accordingly.

$$\tau_w = \frac{6Q\mu}{h^2 w} \tag{2}$$

A summary of experimental parameters can be found in Table 2. For experiments where flow rate is also kept constant (experimental setup 5 and 6), different channel dimensions than setup 1–4 were used to maintain channel aspect ratios of at least 5.

The devices were fabricated using standard soft lithography techniques. Briefly, SU-8 2050 (Microchem, Newton, MA) was spun on a glass slide to the desired channel height. The SU-8 was exposed to UV-light under a photomask of the channels (CAD Art Services, Bandon, OR), and SU-8 developer (Microchem) was applied to remove the uncured SU-8. Channel dimensions were measured with a profilometer to have a deviation from the average of only 3 μm. Polydimethylsiloxane (PDMS) (Dow Corning, Auburn, MI) was mixed at a 10:1 ratio of elastomer to curing agent, and cured for 2 h at 80°C on the mold. The PDMS device was cut from the mold, inlet and outlet holes were punched into the device, and the device was air plasma bonded to a glass slide.

Cell Culture

Osteocyte-like MLO-Y4 cells (a gift from Dr. Lynda Bonewald, Indiana University) were maintained on Collagen-I

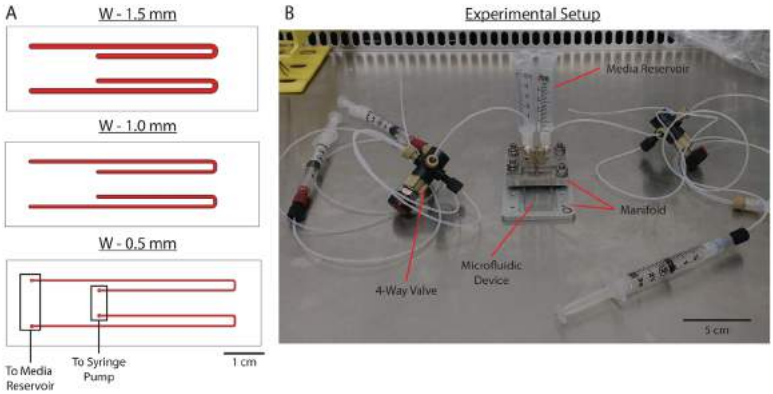

Figure 1. (A) Channel layouts of channels with widths (W) of 1.5, 1.0, and 0.5 mm. Inlet and outlet ports to the syringe pump and waste media reservoir are presented. (B) Experimental setup of the microfluidic device within the manifold.

Table 2. Dimensions and Flow Parameters

Setup #	Re[a]	w (mm)	h (μm)	Q (μl/min)	V_{avg} (cm/s)	μ (10^{-3} Pa·s)	τ (Pa)	$V_{avg} \times \mu$ (10^{-5} Pa·m)
1	1.6 ± 0.2	1.5	50	53.6	1.19	0.7	1	0.83
2	16.8 ± 0.6	1	170	412.9	4.05	0.7	1	2.83
3	2.5 ± 0.3	1.5	50	104.2	2.32	0.9	2.5	2.08
4	25.4 ± 0.8	1	170	802.8	7.87	0.9	2.5	7.08
5	0.29 ± 0.02	1	120	45.7	0.63	4.73	1.5	3.00
6	2.9 ± 0.2	0.5	74	45.7	2.06	0.9	1.5	1.85

[a]Standard deviations calculated based on measured deviations in channel heights of up to 3 μm.

(5% Collagen-I [Corning, Corning, NY], 95% 0.02 N Acetic Acid [Sigma–Aldrich St. Louis, MO]) coated petri dishes (VWR, Radnor, PA). The cells were maintained with MLO-Y4 media consisting of 94% α-MEM (Thermo Fisher Scientific, Waltham, MA), 2.5% Calf Serum (CS) (Thermo Fisher Scientific), 2.5% Fetal Bovine Serum (FBS) (Thermo Fisher Scientific), and 1% Penicillin Streptomycin (P/S) (Thermo Fisher Scientific). Once the cells achieved 80% confluence, the cells were passaged and re-seeded at 300k cells per dish up to passage 40.

Experimental Device Preparation

For experiments, the device was placed into a manifold (Fig. 1B) using techniques previously reported.[23] A detailed description of this setup can be found in the supplemental methods. MLO-Y4 cells were then seeded in the device at a density of 1×10^6 cells/ml and allowed to attach for 2 h at 37°C in an incubator. MLO-Y4 media was added to the reservoir, and perfused (1 μl/min) through the channels for a minimum of 1 day. Afterwards, when the cells reached 80% confluence, flow experiments were performed. Flow rates for each experiment were validated by measuring the displaced volume after the experiment completed.

Cell Spreading Analysis

Cells were imaged at the same locations immediately before and after flow (setup 1 and 2, steady, 1 Pa, 2 h) was applied to the channels. To determine the cell spreading area, images taken across the entire channel width were processed using ImageJ (NIH, Bethesda, MD). First, a threshold was set to the image such that only the cells were highlighted and the "analyze particles" function was used to determine each cell area.

Actin Filament Staining

After flow (setup 1 and 2, steady, 1 Pa, 2 h), the cells were fixed in 3.7% formaldehyde (Sigma–Aldrich) diluted in Dulbecco's phosphate buffered saline (DPBS) (Sigma–Aldrich). The cells were permeabilized with 0.1% Triton-X (Sigma–Aldrich) diluted in DPBS. Actin fibers were stained with Alexa Fluor® 488 Phalloidin (Thermo Fisher Scientific) diluted 1:40 in DPBS, and the nuclei were stained with DAPI (Sigma–Aldrich) diluted 1:1,000 in DPBS. The cells were rinsed with deionized water and fluorescently imaged in the center of the channels. Cells were quantified in terms of cytoskeleton morphology, where "rounded" cells have no extended processes, "elongated" cells have one or two processes, "triangular" cells have three processes, and "dendritic" cells have more than three processes. This type of quantification has previously been applied to osteoblasts and osteocytes undergoing fluid flow.[8] Static channels were prepared as a control.

Apoptosis Analysis

After steady flow (setup 1 and 2, steady, 1 Pa, 2 h), the cells were supplied a perfusion flow (1 μl/min) of media for 2 h. Phase contrast images were taken to determine the total number of cells in the channels. Trypan blue (Sigma–Aldrich) was added to the channels to stain for apoptotic cells as has been previously demonstrated.[24–26] The channels were imaged across the width of the entire channel with bright field microscopy, and apoptotic cells (blue) were counted to determine the percentage of apoptotic cells.

Calcium Staining

To assess mechanosensitivity, we quantified osteocyte intracellular calcium response to different Re flow environments. A Fura-2 AM dye solution was prepared by mixing 50 μg of Fura-2 AM (Thermo Fisher Scientific) with 50 μl of dimethyl sulfoxide (Sigma–Aldrich). This solution was diluted to a final concentration of 10 μM in 5 ml of working media (97% α-MEM without phenol red, 1% FBS, 1% CS, 1% P/S).

The cells were first rinsed with DPBS, and the dye solution was loaded into the channel and allowed to incubate at room temperature for 45 min. The cells were again rinsed with DPBS, and loaded with working media. The device rested on the fluorescent microscope for 30 min before flow was applied. For the experiment, cells were recorded in real-time using Easy-RatioPro (PTI). For 3 min before flow, the cells were ratiometrically imaged (340 nm/380 nm) to determine a baseline of Ca^{2+} signaling. Steady flow (2.5 Pa or 1.5 Pa) was then applied for 3 min, followed by 3 min of no-flow. Calcium measurements from at least 20 cells located at the center of the channel were analyzed using a previously developed MATLAB (MathWorks, Natick, MA) script,[27] which compares calcium peaks after flow started to the maximum peak observed in the baseline region, to quantify the percentage of responding cells and magnitude of the calcium peak. A significant calcium spike was taken to be at least twice the magnitude of the maximum baseline calcium spike.

Three conditions for the calcium experiments were performed. In the first (setup 3 and 4), FSS was kept constant while Re was varied. In the second (setup 5 and 6), both FSS and flow rates were kept constant by modifying the media viscosity using dextran. In the final experiment (setup 5 and 6), FSS and flow rates were again kept constant, but the glycocalyx was degraded to modify osteocyte mechanosensitivity.

Dextran Media

Dextran (500k MW) (Sigma–Aldrich) was mixed in working media to a concentration of 4.7 mg/ml. The viscosity of the dextran media was measured at different shear rates (10–1,000 s^{-1}) using an AR 2000 rheometer (TA Instruments,

New Castle, DE) (courtesy of Dr. David James, University of Toronto), corresponding with a FSS of 0.049–4.8 Pa.

Glycocalyx Degradation

Proteoglycans making up the osteocyte glycocalyx were removed by enzymatic digestion as previously described.[28] Heparinase III from *flavobacterium herparinum* (Sigma–Aldrich) was reconstituted in a solution of 20 mM Tris-HCl (Lonza, Basel, Switzerland), 0.1 mg/ml Bovine Serum Albumin (BioShop, Canada, Inc., Burlington, Ontario, Canada), and 4 mM $CaCl_2$ (Sigma–Aldrich) to a concentration of 20 U/ml. This was further diluted in MLO-Y4 media to a final concentration of 0.4 U/ml. The enzyme solution was applied to osteocytes in the microfluidic channel for at least 2 h before the experiment to remove Heparan Sulfates (HS).

To validate that HS was degraded, we stained cells with or without exposure to Heparinase III with Wheat Germ Agglutinin (WGA) conjugated with Alexa Fluor® 488 (Thermo Fisher Scientific). A stock solution of WGA (1 mg/ml) was diluted in Hank's Balanced Salt Solution (HBSS) (Thermo Fisher Scientific) without phenol red to a concentration of 5 μg/ml. The staining solution was added to the cells for 10 min at 37°C. The cells were rinsed two times with DPBS and fluorescently imaged. Cell fluorescent intensities were quantified in ImageJ after subtracting the background intensity.

Statistics

The student *t*-test was performed on the cell spreading, apoptosis, calcium, and enzyme digestion data. One-way ANOVA was performed on the actin data, followed by a pair-wise *t*-test. Finally, the Holm–Bonferroni method was applied to the actin and calcium data to account for multiple comparisons. Statistical significance was taken at $\alpha = 0.05$.

RESULTS

Cell Spreading Area

Before flow, the MLO-Y4 cells displayed their characteristic dendritic morphology (Fig. 2A and C). After flow, cells exposed to a higher *Re* flow maintained their morphology (Fig. 2D), while those exposed to a lower *Re* flow became rounded (Fig. 2B). Quantification of cell spreading area confirmed this observation, as the higher *Re* cells had no significant change in cell spreading, while the lower *Re* cells had a 14% reduction in cell spreading area (Fig. 2E).

Actin Filament

Characteristic images of the actin filaments with or without FSS are presented in Figures 3A–C. Upon quantification of the actin morphologies, we observed that, given a higher *Re* flow, there was a 79% increase in the percentage of "triangular" cells, and a 36% reduction in the percentage of "elongated" cells relative to the static control (Fig. 3D). When exposed to a lower *Re* flow, we observed a 111% increase in the

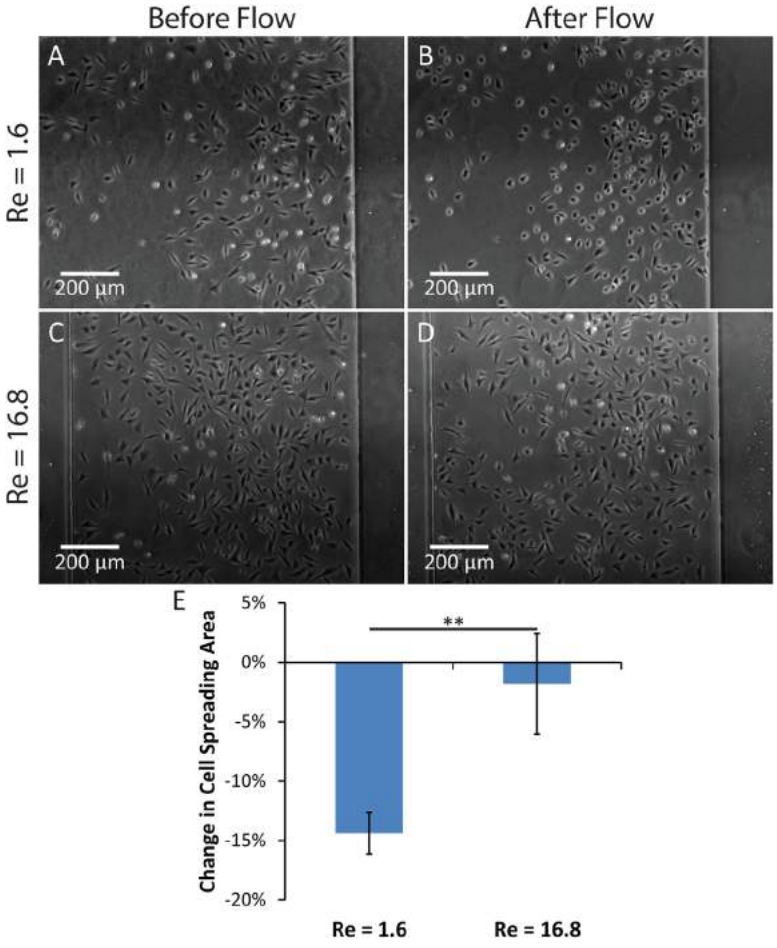

Figure 2. Phase contrast images of MLO-Y4 cells in (A, B) low *Re* and (C, D) high *Re* (C,D) microfluidic channels (A, C) before and (B, D) after flow. (E) Quantification of change of area from ImageJ. Error bars are one standard deviation. $N = 4$ for lower *Re* and $N = 3$ for higher *Re*. $^{**}p < 0.01$.

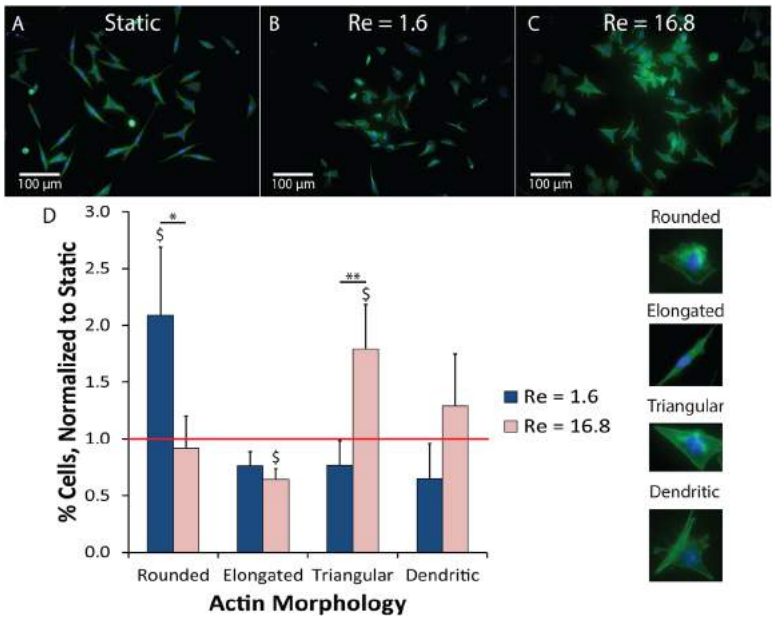

Figure 3. Actin filament staining of MLO-Y4 cells (A) before and (B, C) after 2 h of 1 Pa fluid shear stress given (B) lower and (C) higher *Re* flows. (D) Plot of proportion of different cytoskeletal morphologies after exposure to lower and higher *Re* flows normalized to static (signified by the red line). $N = 4$ for higher *Re* and $N = 3$ for lower *Re* and static. Error bars are one standard deviation as calculated by propagation of error. $^{\$}p < 0.05$ compared to static.* $p < 0.05$, $^{**}p < 0.01$ for comparisons between lower and higher *Re*.

percentage of "rounded" cells relative to static (Fig. 3D).

Apoptosis

After flow, we observed low apoptosis rates in both microfluidic channels (<10%). We also observed that cells exposed to the lower *Re* flow had a significantly lower apoptosis rate (3%) compared to those exposed to a higher *Re* flow (7%) (Fig. 4).

Intracellular Calcium Response

Shear Stress Constant

When only FSS was held constant, we observed no difference in the percentage of responding cells between the two *Re* flow environments (Fig. 5A). However, the magnitude of the response was increased for the higher *Re* flow (4.3×) than the lower *Re* flow (2.8×) (Fig. 5B).

Shear Stress and Flow Rate Constant

We measured that the viscosity of the dextran media was 4.73×10^{-3} Pa·s and independent of shear rate (Fig. 6A). When both flow rate and FSS were kept constant, an increased percentage of cells responded to the lower *Re* flow (88%) than the higher *Re* flow (30%) (Fig. 6B). We similarly observed that the magnitude of the response was stronger for cells exposed to the lower *Re* flow (4.3×) than the higher *Re* flow (2.5×) (Fig. 6C).

Shear Stress and Flow Rate Constant—HS Digested

After digestion, we observed a 42% decrease in fluorescent intensity relative to the background (Fig. 7A). The remnant fluorescence is likely due to WGA binding to Hyaluronic Acid, which was not digested.[29] After digestion, we observed that there was no difference in the percentage of responding cells given either *Re* flow environment (Fig. 7B). However, we did observe an increased magnitude of response given a higher *Re* flow (5.4×) compared to a lower *Re* flow (3.2×) (Fig. 7C).

DISCUSSION

For a scale model to be a valid representation of the real-world system, the two must have dynamic similarity in the flow environment, thereby requiring the same *Re*. However, despite its prevalence in various industries, this concept of dynamic similarity has yet to be significantly applied to in vitro models of biological fluid systems. To elucidate the role that the *Re* regulated flow environment plays in cell mechanotransduction, we utilized different dimensioned microfluidic channels to generate different *Re* flows while keeping other fluid flow parameters constant. As well, the small entrance lengths of these channels (order of microns) allowed for the mitigation of a significant limitation of PPFCs, where a significant area of the chambers do not undergo fully developed flow.[30] We

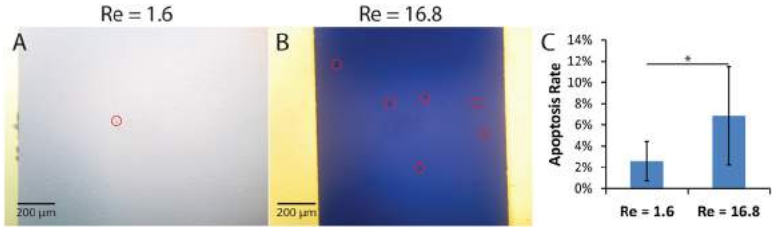

Figure 4. Characteristic bright field images of MLO-Y4 cells stained with Trypan Blue in the (A) lower and (B) higher *Re* channels. Circles identify positively stained cells. Different intensity in channel color is due to differences in channel heights. (C) Quantification of apoptosis rates in both the lower and higher *Re* channels. Error bars signify one standard deviation. $N = 5$ for the lower *Re* channel and $N = 8$ for the higher *Re* channel. $^{*}p < 0.05$.

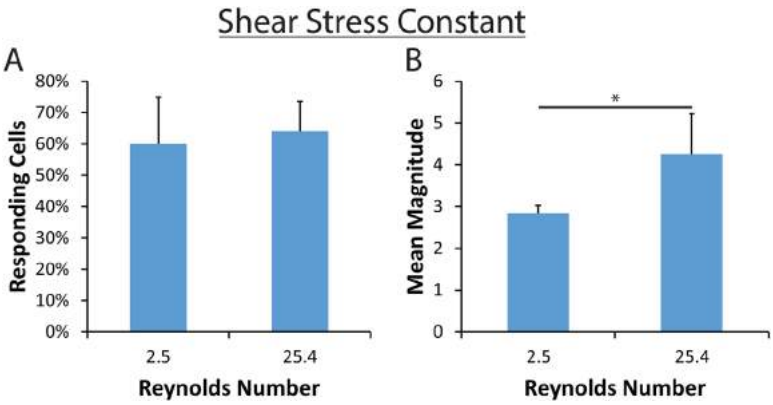

Figure 5. (A) Percentage of imaged cells that had a calcium response of at least twice the baseline and (B) average magnitude of the calcium spike of the responding cells when only shear stress is kept constant at different *Re*. $N = 5$. Error bars are one standard deviation. $^{*}p < 0.05$.

used osteocytes, the main mechanosensory cells in bone,[31] to investigate how different *Re* flow environments affected cell morphology, actin filament rearrangement, apoptosis rate, and intracellular calcium expression. This study is the first time that the *Re* has been used to control the flow environment and investigate its effect on osteocyte mechanoresponse.

Under a lower *Re* flow, we first observed a significant reduction in cell spreading area that was not observed given a higher *Re* flow (Fig. 2). Similarly, when we stained for actin, we observed that osteocytes tend to lose their dendritic appearance and switch to a "rounded" morphology given a lower *Re* flow, while, under a higher *Re* flow, the cells tend to develop a predominantly 'triangular' morphology (Fig. 3). One method osteocytes respond to flow is the upregulation of E11/gp38 mRNA,[32] which promotes process formation and lengthening.[33] As well, it has been demonstrated that the application of FSS to osteocytes stimulates actin filament reorganization,[8] which controls the morphology and shape of the cell body and processes.[34] Although this result suggests that osteocytes are sensitive to dynamic differences in the flow environment besides shear stress, the question remains through what mechanism this response occurs. Since *Re* is defined as a ratio of dynamic pressure to shear stresses, and since we keep shear stresses constant within experimental groups, increasing dynamic pressure by increasing *Re* could induce this response as volume modulating forces have been demonstrated to stimulate cytoskeletal reorganization.[5] It has also been previously suggested that chemotransport regulates bone cell mechanosensitivity.[7] In this experimental setup (setup 1 and 2), osteocytes exposed to higher *Re* flows undergo flow rates that are 8 times larger than those experiencing the lower *Re* flow. It has been speculated that low chemotransport results in a buildup of waste products and/or a lack of adequate nutrient replacement that could result in decreased cellular mechanosensitivity.[6] Although this chemotransport effect exists in vitro, it is unlikely to be significant physiologically, where applied flow rates are significantly lower,[16] as fluid mixing in the LCS due to oscillatory flow allows for sufficient nutrient supply.[35]

To assess whether a decrease in chemotransport in the lower *Re* experiments would affect cell viability, we quantified cell apoptosis after flow. After exposure to either *Re* flow environment, osteocytes were observed to have low apoptosis rates (<10%). Furthermore, the apoptosis rate in the higher *Re* experiment was larger than observed given a lower *Re* flow (Fig. 4). This result suggests that the observed cell rounding was not due to cell apoptosis. However, it is unclear why the higher *Re* flow environments are inducing increased rates of apoptosis, and further investigation is needed to understand the mechanisms involved.

To assess the mechanosensitivity of osteocytes given different *Re* flow environments, we investigated their intracellular calcium response. When osteocytes are mechanically stimulated, calcium enters the cell cytosol from both the endoplasmic reticulum and the surrounding extracellular fluid.[12] When only FSS was kept constant, we observed that osteocytes exposed to a higher *Re* flow had an increase in the calcium peak magnitude (Fig. 5B), supporting our previous observation that osteocytes exposed to a higher *Re* flow are more mechanosensitive.

Since flow rate was identified as a potential regulator of osteocyte response to the flow environment, we next kept both the FSS and flow rate constant. We

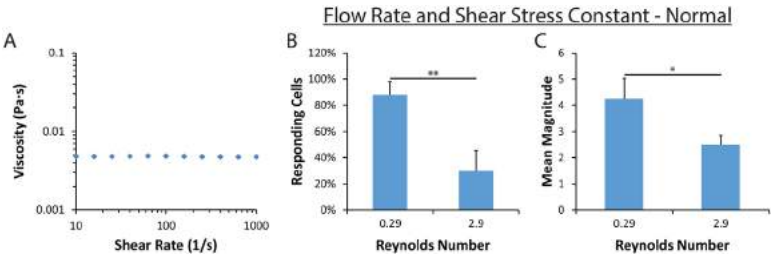

Figure 6. (A) Dextran media viscosity at different shear rates. $N = 5$. (B) Percentage of cells responding with a calcium peak of at least two times the maximum baseline response and (C) the mean magnitude of the calcium response of the responding cells when flow rate is also kept constant using a dextran media. $N = 4$. Error bars are on standard deviation. $^{*}p < 0.05$, $^{**}p < 0.01$.

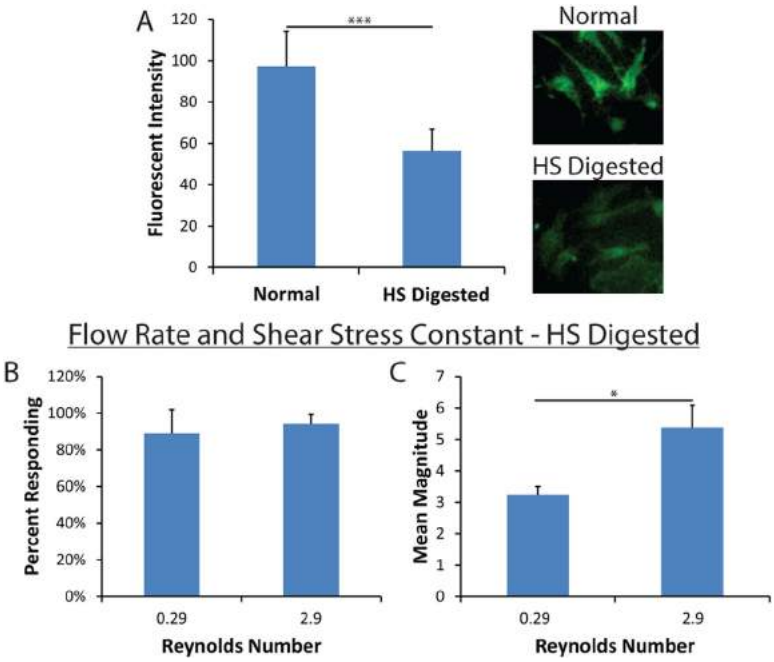

Figure 7. (A) Plot of cell fluorescent intensities relative to the background, as well as characteristic images of normal and HS digested osteocytes after WGA staining. $N = 6$. (B) Percentage of cells responding with a calcium peak of at least two times the maximum baseline response. (C) The mean magnitude of the calcium response of the responding cells after digestion of HS when flow rate and shear stress are kept constant. $N = 3$. Error bars are one standard deviation. $^{*}p < 0.05$, $^{***}p < 0.001$.

observed that osteocytes exposed to a lower *Re* flow demonstrated significant increases in both the percentage of responding cells (Fig. 6B) and mean magnitude of the response (Fig. 6C). This result demonstrates the importance that flow rate has on regulating osteocyte mechanosensitivity. As well, since the higher *Re* flow also has an increased dynamic pressure, this suggests that flow rate has a more significant role in regulating osteocyte mechanosensitivity. However, since a difference still exists in osteocyte mechanoresponse, another mechanism likely exists through which osteocytes sense their specific *Re* flow environment. Due to the high fluid viscosity used in the lower *Re* channel, we suspected that osteocytes were sensing this viscous force through mechanisms other than FSS, such as drag forces applied to the osteocyte glycocalyx.

It has been established that the osteocyte glycocalyx regulates various osteocyte mechanoresponses[29,36] and its degradation in vivo significantly impacts bones response to flow.[37] It has been suggested that the dominant force experienced by osteocytes in vivo comes from drag forces (caused by cellular elements that resist fluid flow) as opposed to shearing forces.[37–39] Furthermore, in endothelial cells, it has been modeled that the drag stresses applied to the glycocalyx are proportional to the fluid viscosity and superficial fluid velocity.[40] When we multiplied the viscosity and velocity for each experimental condition (Table 2), we observed that increases in this value corresponded with an increased mechanoresponse.

To understand the role of the osteocyte glycocalyx in mechanosensation, we investigated osteocyte calcium responses to flow after degradation of HS. We observed that digestion of HS resulted in an increase in the magnitude of the response to a higher *Re* flow (Fig. 7C), suggesting a decreased effect of drag forces on osteocyte mechanosensitivity. Analytical modeling[38] of the osteocyte pericellular matrix suggested that digestion of the osteocyte glycocalyx would decrease the force ratio (drag force/shear force) due to increased fiber spacing, potentially explaining the reduced relative calcium response when exposed to a lower *Re* flow. Previous research on the osteocyte glycocalyx has also demonstrated that it is critical in the formation of mechanosensory integrins.[41] Furthermore, it has been demonstrated that degradation of the glycocalyx reduced osteocytes Prostaglandin E2 response to FSS.[29] However, that study did not observe any effect on calcium signaling after degradation, which the author postulated was due to equal and opposite effects of glycocalyx degradation on the cell surface FSS and drag force applied.[29] Due to different conditions in our experiments, this balance between surface FSS and drag force has likely been affected. Regardless, more investigation is clearly needed to study the role of the glycocalyx on osteocyte mechanosensitivity.

Although this work demonstrated the *Re* dependency of osteocytes mechanosensitivity to fluid flow through various mechanisms, there are some limitations to this study. First, the range of *Re* of the flow environments that were investigated are still orders of magnitude larger than physiological. To produce relevant *Re* in vitro, channel hydraulic diameters must be reduced and/or fluid viscosities must be increased. Additionally, we only indirectly quantified the shear stresses (by setting the flow rate) applied to the osteocytes. By utilizing advanced flow imaging techniques, such as micro-particle image velocimetry, we could more accurately measure the specific stresses applied to the cells.[42] A further limitation is that this is a 2D model of a 3D system. A critical component of osteocyte mechanosensation in vivo is the formation of

cellular attachments to the canalicular wall.[38] Microscale platforms have recently been developed to better mimic the dimensions and orientation of the LCS.[43,44] Although these platforms have yet to be utilized to study osteocyte mechanotransduction, flow studies using these platforms could provide more physiologically relevant data. Similarly, aberrations in the pericanalicular space have been suggested to produce localized regions of concentrated stresses on osteocyte processes,[45,46] higher than what is currently measured. Future enhancements of microfluidics technologies could allow for the incorporation of fluid stress concentrators to further increase the relevance of these studies.

This study is the first time that osteocyte mechanosensitivity dependency on dimensional modifications of their flow environments, the *Re* number, is investigated in vitro. In this study, we identified that flow environments with different *Re* numbers regulated osteocyte mechanoresponses in terms of morphology, cytoskeleton organization, apoptosis rate, and calcium response. We identified that these differing responses were, at least in part, due to differences in flow rates and drag forces acting on the cells. Furthermore, sensitivity to these parameters can potentially explain differences in osteocyte mechanoresponses observed by different labs in the bone mechanobiology community, and highlights the need for incorporating constantly improving microfluidic platforms into in vitro bone cell research. This type of study could also be applied to other mechanosensitive cells, such as endothelial cells, which are typically studied using PPFCs.

AUTHORS' CONTRIBUTIONS

KM assisted with device and experimental design, performed a significant amount of the experimentation and data analysis, and prepared the manuscript. AK performed experimental design, performed significant experimentation, and helped with the manuscript. MB performed significant device design and preliminary experimental design. YC helped with experimental design and significantly helped with experimentation. XM significantly helped with experimentation. LY supervised the study, significantly helped with experimental design and analysis of results, as well as providing significant input in editing the manuscript. All authors approve of the contents of the manuscript.

ACKNOWLEDGMENTS

We acknowledge postgraduate research funding from the Natural Sciences and Engineering Research Council, the Toronto Musculoskeletal Centre, and Barbara and Frank Milligan. Funding for this research was provided by the Canadian Institutes of Health Research (fund #282723). Microfluidic fabrication facilities were provided by the Centre for Microfluidic Systems in Chemistry and Biology at the University of Toronto that is funded by the Canada Foundation for Innovation and the Ontario Research Fund.

REFERENCES

1. Resnick N, Yahav H, Shay-Salit A, et al. 2003. Fluid shear stress and the vascular endothelium: for better and for worse. Prog Biophys Mol Biol 81:177–199.
2. Riddle RC, Donahue HJ. 2009. From streaming potentials to shear stress: 25 Years of bone cell mechanotransduction. J Orthop Res 27:143–149.
3. Li J, Rose E, Frances D, et al. 2012. Effect of oscillating fluid flow stimulation on osteocyte mRNA expression. J Biomech 45:247–251.
4. Sheikh S, Rainger GE, Gale Z, et al. 2003. Exposure to fluid shear stress modulates the ability of endothelial cells to recruit neutrophils in response to tumor necrosis factor-α: a basis for local variations in vascular sensitivity to inflammation. Blood 102:2828–2834.
5. Chang H, Knothe Tate ML. 2011. Structure-function relationships in the stem cell's mechanical world B: emergent anisotropy of the cytoskeleton correlates to volume and shape changing stress exposure. Mol Cell Biomech 8:297–318.
6. Donahue TLH, Haut TR, Yellowley CE, et al. 2003. Mechanosensitivity of bone cells to oscillating fluid flow induced shear stress may be modulated by chemotransport. J Biomech 36:1363–1371.
7. Riddle RC, Hippe KR, Donahue HJ. 2008. Chemotransport contributes to the effect of oscillatory fluid flow on human bone marrow stromal cell proliferation. J Orthop Res 26:918–924.
8. Ponik SM, Triplett JW, Pavalko FM. 2007. Osteoblasts and osteocytes respond differently to oscillatory and unidirectional fluid flow profiles. J Cell Biochem 100:794–807.
9. Jacobs CR, Yellowley CE, Davis BR, et al. 1998. Differential effect of steady versus oscillating flow on bone cells. J Biomech 31:969–976.
10. Lu XL, Huo B, Park M, et al. 2012. Calcium response in osteocytic networks under steady and oscillatory fluid flow. Bone 51:466–473.
11. Anderson EJ, Kreuzer SM, Small O, et al. 2008. Pairing computational and scaled physical models to determine permeability as a measure of cellular communication in micro- and nano-scale pericellular spaces. Microfluid Nanofluidics 4:193–204.
12. Lu XL, Huo B, Chiang V, et al. 2012. Osteocytic network is more responsive in calcium signaling than osteoblastic network under fluid flow. J Bone Miner Res 27:563–574.
13. Robling AG, Niziolek PJ, Baldridge LA, et al. 2008. Mechanical stimulation of bone in vivo reduces osteocyte expression of sost/sclerostin. J Biol Chem 283:5866–5875.
14. Nakashima T, Hayashi M, Fukunaga T, et al. 2011. Evidence for osteocyte regulation of bone homeostasis through RANKL expression. Nat Med 17:1231–1234.
15. Kulkarni RN, Bakker AD, Everts V, et al. 2010. Inhibition of osteoclastogenesis by mechanically loaded osteocytes: involvement of MEPE. Calcif Tissue Int 87:461–468.
16. Price C, Zhou X, Li W, et al. 2011. Real-time measurement of solute transport within the lacunar-canalicular system of mechanically loaded bone: direct evidence for load-induced fluid flow. J Bone Miner Res 26:277–285.
17. You L-D, Weinbaum S, Cowin SC, et al. 2004. Ultrastructure of the osteocyte process and its pericellular matrix. Anat Rec A Disc Mol Cell Evol Biol 278A:505–513.
18. Jing D, Baik AD, Lu XL, et al. 2014. In situ intracellular calcium oscillations in osteocytes in intact mouse long bones under dynamic mechanical loading. FASEB J 28:1582–1592.
19. Zhang J-N, Zhao Y, Liu C, et al. 2015. The role of the sphingosine-1-phosphate signaling pathway in osteocyte mechanotransduction. Bone 79:71–78.

20. Yu W, Qu H, Hu G, et al. 2014. A microfluidic-based multi-shear device for investigating the effects of low fluid-induced stresses on osteoblasts. PLoS ONE 9:e89966.
21. Zhong W, Tian K, Zheng X, et al. 2013. Mesenchymal stem cell and chondrocyte fates in a multishear microdevice are regulated by yes-associated protein. Stem Cells Dev 22:2083–2093.
22. Kou S, Pan L, van Noort D, et al. 2011. A multishear microfluidic device for quantitative analysis of calcium dynamics in osteoblasts. Biochem Biophys Res Commun 408:350–355.
23. Middleton K, Al-Dujaili S, Mei X, et al. 2017. Microfluidic co-culture platform for investigating osteocyte-osteoclast signalling during fluid shear stress mechanostimulation. J Biomech 59:35–42.
24. Ahuja SS, Zhao S, Bellido T, et al. 2003. CD40 ligand blocks apoptosis induced by tumor necrosis factor alpha, glucocorticoids, and etoposide in osteoblasts and the osteocyte-like cell line murine long bone osteocyte- Y4. Endocrinology 144: 1761–1769.
25. Kitase Y, Barragan L, Qing H, et al. 2010. Mechanical induction of PGE2 in osteocytes blocks glucocorticoid-induced apoptosis through both the beta-catenin and PKA pathways. J Bone Miner Res 25:2657–2668.
26. Jahn K, Lara-Castillo N, Brotto L, et al. 2012. Skeletal muscle secreted factors prevent glucocorticoid-induced osteocyte apoptosis through activation of beta-catenin. Eur Cell Mater 24:197–209.
27. Liu C, Zhao Y, Cheung W-Y, et al. 2010. Effects of cyclic hydraulic pressure on osteocytes. Bone 46:1449–1456.
28. Zeng Y, Ebong EE, Fu BM, et al. 2012. The structural stability of the endothelial glycocalyx after enzymatic removal of glycosaminoglycans. PLoS ONE 7:e43168.
29. Reilly GC, Haut TR, Yellowley CE, et al. 2003. Fluid flow induced PGE2 release by bone cells is reduced by glycocalyx degradation whereas calcium signals are not. Biorheology 40:591–603.
30. Anderson EJ, Falls TD, Sorkin AM, et al. 2006. The imperative for controlled mechanical stresses in unraveling cellular mechanisms of mechanotransduction. Biomed Eng Online 5:27.
31. Bonewald LF, Johnson ML. 2008. Osteocytes, mechanosensing and Wnt signaling. Bone 42:606–615.
32. Zhang K, Barragan-Adjemian C, Ye L, et al. 2006. E11/gp38 selective expression in osteocytes: regulation by mechanical strain and role in dendrite elongation. Mol Cell Biol 26:4539–4552.
33. Bonewald LF. 2007. Osteocytes as dynamic multifunctional cells. Ann NY Acad Sci 1116:281–290.
34. Tanaka-Kamioka K, Kamioka H, Ris H, et al. 1998. Osteocyte shape is dependent on actin filaments and osteocyte processes are unique actin-rich projections. J Bone Miner Res 13:1555–1568.
35. Wang L, Cowin SC, Weinbaum S, et al. 2000. Modeling tracer transport in an osteon under cyclic loading. Ann Biomed Eng 28:1200–1209.
36. Burra S, Nicolella DP, Jiang JX. 2011. Dark horse in osteocyte biology: glycocalyx around the dendrites is critical for osteocyte mechanosensing. Commun Integr Biol 4:48–50.
37. Wang B, Lai X, Price C, et al. 2014. Perlecan-containing pericellular matrix regulates solute transport and mechanosensing within the osteocyte lacunar-canalicular system. J Bone Miner Res 29:878–891.
38. You L, Cowin SC, Schaffler MB, et al. 2001. A model for strain amplification in the actin cytoskeleton of osteocytes due to fluid drag on pericellular matrix. J Biomech 34:1375–1386.
39. Fan L, Pei S, Lucas Lu X, et al. 2016. A multiscale 3D finite element analysis of fluid/solute transport in mechanically loaded bone. Bone Res 4:16032.
40. Tarbell JM, Shi ZD. 2013. Effect of the glycocalyx layer on transmission of interstitial flow shear stress to embedded cells. Biomech Model Mechanobiol 12:111–121.
41. Burra S, Nicolella DP, Francis WL, et al. 2010. Dendritic processes of osteocytes are mechanotransducers that induce the opening of hemichannels. Proc Natl Acad Sci USA 107:13648–13653.
42. Song MJ, Brady-Kalnay SM, McBride SH, et al. 2012. Mapping the mechanome of live stem cells using a novel method to measure local strain fields in situ at the fluid-cell interface. PLoS ONE 7:43601.
43. You L, Temiyasathit S, Tao E, et al. 2008. 3D microfluidic approach to mechanical stimulation of osteocyte processes. Cell Mol Bioeng 1:103–107.
44. Sun Q, Gu Y, Zhang W, et al. 2015. Ex vivo 3D osteocyte network construction with primary murine bone cells. Bone Res 3:15026.
45. Anderson EJ, Knothe Tate ML. 2008. Idealization of pericellular fluid space geometry and dimension results in a profound underprediction of nano-microscale stresses imparted by fluid drag on osteocytes. J Biomech 41: 1736–1746.
46. Kamioka H, Kameo Y, Imai Y, et al. 2012. Microscale fluid flow analysis in a human osteocyte canaliculus using a realistic high-resolution image-based three-dimensional model. Integr Biol 4:1198–1206.

SUPPORTING INFORMATION

Additional supporting information may be found in the online version of this article.